Chapter 11
Requirements on Periodic Micromorphic Media

Ralf Jänicke and Stefan Diebels

Abstract In order to investigate the properties of microstructured materials, the underlying heterogeneous material is commonly replaced by a homogeneous material involving additional degrees of freedom. Making use of an appropriate homogenization methodology, the present contribution compares deformation states predicted by the homogenization technique to the deformation state within a reference solution. The results indicate on what terms the predicted deformation modes can be clearly interpreted from the physical point of view.

11.1 Introduction

Microstructured materials are known to feature a complex mechanical behavior which is strongly dominated by the underlying microtopology. A well documented phenomenon is the stiff boundary layer effect inducing size-dependent effective material properties, e.g., [2, 17, 18]. In the literature, various approaches exist which replace the heterogeneous microcontinuum by a homogeneous macrocontinuum, enriched by additional degrees of freedom. A wide range of those approaches goes back to the fundamental considerations of the Cosserat brothers[1], and these considerations were systematically generalized by Eringen [3]. Different approaches deal with second gradient media, e.g., [8, 11, 14]. During the last decade, considerable advances in the numerical modeling of microstructured materials took place, namely by using the so-called two-level FEM or FE^2 approaches, e.g., [4, 11, 15].

In the present contribution, we make use of a second order homogenization procedure introduced in detail in [10]. For this purpose, the kinematic quantities are

R. Jänicke (✉) · S. Diebels

Chair of Applied Mechanics, Saarland University, Campus A 4.2, 66123 Saarbrücken, Germany
e-mail: r.jaenicke@mx.uni-saarland.de

S. Diebels
e-mail: s.diebels@mx.uni-saarland.de

expressed in terms of a polynomial mean field and a periodic fluctuation on a microvolume attached to the macroscopic material point. After having reviewed the scale transition of the kinematic quantities, several numerical experiments will help analyze the significance of the deformation modes involved in the proposed approach in comparison to a reference solution. Special attention will be paid to the methodology's requirements on the attached microvolume.

11.2 Micromorphic Media

The physical picture Following the seminal works of Eringen [3], we assume the physical body $\mathscr{B}_M$ to consist of a set of deformable material points which capture a small but finite space $\mathscr{B}_m$. The microcontinuum's mapping from the material to the spatial frame is considered to be affine and reads

$$\Delta \mathbf{x}(\mathbf{X}_M, \overline{\chi}_M, t) = \overline{\chi}_M(\mathbf{X}_M, t) \cdot \Delta \mathbf{X}(\mathbf{X}_M). \qquad (11.1)$$

$\overline{\chi}_M$ is defined as the microdeformation tensor, the index $(\diamond)_M$ refers to the macroscale and $(\diamond)_m$ to the microscale, respectively. By calculating the square of the deformed arc length $(\mathrm{d}\mathbf{x}_m)^2$, one has to introduce a set of three independent deformation measures. Without loss of generality, we choose the common deformation gradient $\mathbf{F}_M$, the microdeformation $\overline{\chi}_M$ and its gradient $\mathrm{Grad}\,\overline{\chi}_M$. Obviously, this set of two-field quantities does not fulfill the requirements of objectivity. Nevertheless, the given set is admissible for the following investigations because no constitutive assumptions will be met.

Scale transition of the kinematic quantities   In the sequel, a consistent averaging technique will be sketched replacing a heterogeneous Cauchy medium, representing the cellular network, by a homogeneous micromorphic medium. Based on a methodology proposed by Forest and Sab [5, 7] and presented in detail in [10], one can identify the kinematic quantities of the micromorphic macrocontinuum in terms of a polynomial mean field and a periodic perturbation of the heterogeneous Cauchy microcontinuum attached to the micromorphic material point on the macroscale. To simplify matters, the attached microvolume is assumed to be a rhombic unit cell as
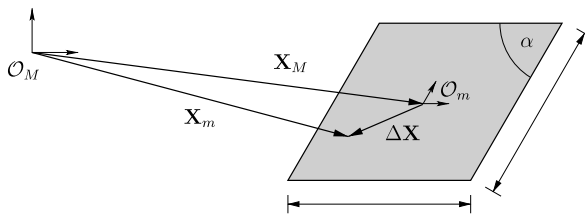

Fig. 11.1 The attached rhombic microvolume representing the cellular network. The volume centroid of $\mathscr{B}_m$ is defined by the position vector $\mathbf{X}_M$ (material frame)

depicted in Fig. 11.1. We postulate the set $(\mathbf{u}_M, \overline{\chi}_M)$ to characterize the macrostate that best fits the microscopic displacement field $\mathbf{u}_m$ in an averaged sense. Thus, we minimize the functional

$$\mathscr{F}(\mathbf{u}_M, \overline{\chi}_M) = \left\langle (\mathbf{u}_m - \mathbf{u}_M - (\overline{\chi}_M - \mathbf{I}) \cdot \Delta\mathbf{X})^2 \right\rangle \qquad (11.2)$$

with the volume average $\langle \diamond \rangle = 1/V_m \int_{\mathscr{B}_M} \diamond \, \mathrm{d}V_m$ and we find

$$\langle \Delta\mathbf{u} \rangle = \mathbf{0} \quad \text{and} \quad \overline{\chi}_M = \langle \mathbf{u}_m \otimes \Delta\mathbf{X} \rangle \cdot \mathbf{G}^{-1} + \mathbf{I}, \qquad (11.3)$$

where $\mathbf{G}$ is a second order geometry tensor defined by the shape of the attached microvolume. Assuming a microscopic displacement field as a polynomial of grade three, one can show that the expression

$$\Delta\mathbf{x} = \mathbf{F}_M \cdot \Delta\mathbf{X} + \frac{1}{2} \operatorname{Grad} \overline{\chi}_M : (\Delta\mathbf{X} \otimes \Delta\mathbf{X})$$

$$+ \frac{1}{6} \overset{*}{\chi}_M \cdot \mathbf{G}^{\underline{4}} \vdots (\Delta\mathbf{X} \otimes \Delta\mathbf{X} \otimes \Delta\mathbf{X}) + \Delta\tilde{\mathbf{x}} \qquad (11.4)$$

satisfies the averaging rules of (11.3), where a fourth order geometry tensor $\mathbf{G}^{\underline{4}}$ depending on the microvolume's shape has been introduced and where the difference $\overset{*}{\chi}_M = \overline{\chi}_M - \mathbf{F}_M$ has been used as an independent quantity. $\Delta\tilde{\mathbf{x}}$ represents a fluctuation field due to the microstructural periodicity. Having in mind the linear displacement field $\Delta\mathbf{x} = \mathbf{F}_M \cdot \Delta\mathbf{X} + \Delta\tilde{\mathbf{x}}$ of a so-called first-order FE^2 approach replacing a heterogeneous Cauchy microcontinuum by a homogeneous Cauchy macrocontinuum, (11.4) is pointing out the extended character of the introduced projection rule. Equation (11.4) clearly indicates the restricted character of the cubic projection link. For the 2D case, there only exist 4 independent cubic deformation modes in contrast to an unrestricted cubic polynomial allowing for 8 independent cubic deformation modes. In the sequel, the significance of the higher order deformation modes, i.e., quadratic and cubic ones, will be investigated for several perfectly periodic microstructures.

11.3 Higher Order Deformation Modes in Periodic Microstructures

The substitution of a heterogeneous microcontinuum by an extended but homogeneous macrocontinuum requires the additional macroscopic degrees of freedom to display the real deformation mechanisms of the microstructure in an adequate way. As it has been shown in the precedent section, the micromorphic kinematics enrich the microscopic displacement field by quadratic and cubic parts. In order to determine the relevance of these higher order deformation modes, a set of four perfectly periodic microstructures is subject to several numerical experiments. The analyzed
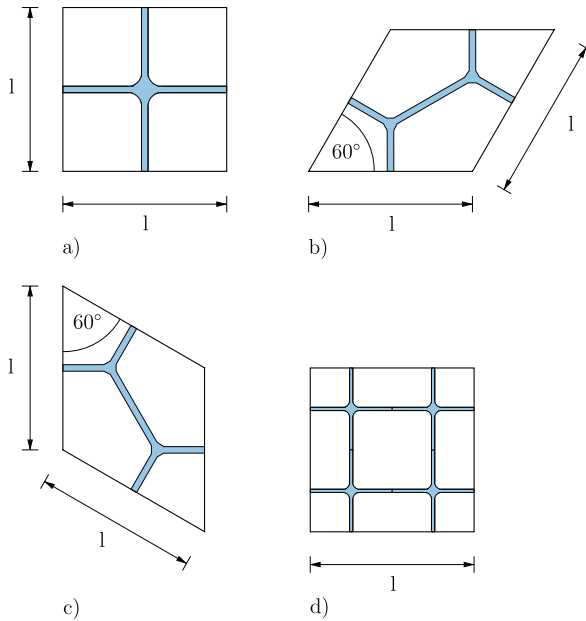
Fig. 11.2 The periodic unit cells of the investigated cellular microstructures. The structures are considered as lattices of struts which are rigidly connected in vertices. The interaction between two vertices only depends on the geometry and the material properties of the connecting struts. Microstructure (*a*) represents an 1-particle system, whereas microstructures (*b*) and (*c*) involve 2 particles, microstructure (*d*) 4 particles, respectively. The struts feature an aspect ratio $r \approx 1/20$ for (*a*) and (*d*), $r \approx 1/12$ for (*b*) and (*c*), respectively

periodic unit cells are depicted in Fig. 11.2. The given microstructures can be considered as lattices of struts which are rigidly connected in vertices. Thus, the material properties and the geometry of the struts control the interaction between two joined vertices. In analogy to systems consisting of discrete particles interacting via their boundary, one may interpret the vertices as particles and the given microstructures as n-particle systems, cf. [16], scaling n from 1 to 4. Thus, n involves the number of particles within the periodic unit cell. The experimental setup is depicted in Fig. 11.3 in a schematic way for microstructure (a) and has been accomplished in an analogous way for the microstructures (b)–(d), i.e., the particular microstructures have been microscopically resolved by finite elements. The performed deformations are assumed to be small. The cell walls follow Hooke's law.

At 4 different positions ① – ④ of the numerical experiments, the displacement field on the boundary of the labeled unit cell embedded in the microscopically resolved cellular structure is observed. In order to determine how accurate this real displacement field can be reproduced by the projection rule in (11.4), several projection polynomials have been fitted to the observed displacement field using the method of least squares. The study comprises a linear polynomial (4 independent deformation modes) in analogy to a first order FE^2 approach, a quadratic polyno-
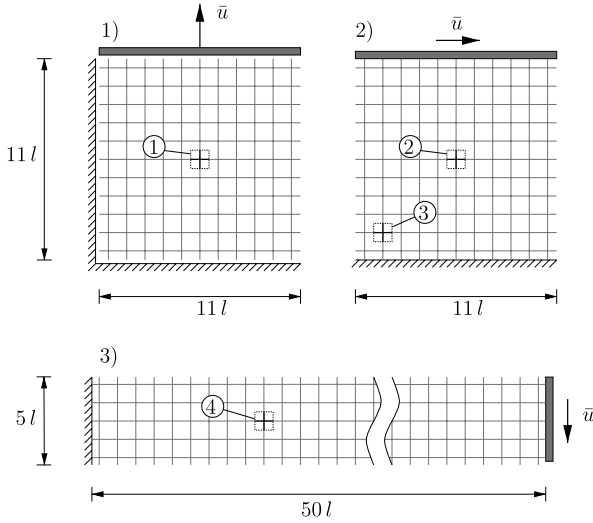
Fig. 11.3 Setup of the numerical experiments: (**1**) homogeneous tension test, (**2**) inhomogeneous shear test, (**3**) bending test, exemplary displayed for microstructure (*a*), microstructures (*b*)–(*d*) analogously. The struts are microscopically resolved by finite elements and follow Hooke's law (Young's modulus $Y = 200$ GPa, Poisson's ratio $\nu = 0.33$). The embedded unit cells subject to the further investigations are denoted with ① – ④

mial ($4 + 6 = 10$ independent deformation modes) in analogy to a second order FE^2 approach using a second-gradient continuum on the macroscale, e.g., [11, 12], a micromorphic polynomial ($4 + 6 + 4 = 14$ independent deformation modes) as introduced earlier, and finally an unrestricted cubic one ($4+6+8 = 18$ independent deformation modes). Note that the fitting procedure is up to the well-defined polynomial orders. Thus, no periodic fluctuations are taken into account. In Figs. 11.4–11.7, the observed least squares of the fitted displacement field normalized to the linear one is plotted over the number of independent deformation modes.

11.4 Discussion

Considering Figs. 11.4–11.7, one may generally notice several points of interest:

- The increase in the fitting polynomial from a linear to a cubic one involves a decrease in the error over several orders of magnitude for the cross-like microstructure (a). In a less distinct manner, the same correlation holds for the honeycomb unit cells (b) and (c). Obviously, this is not the case for microstructure (d) showing the same symmetry as (a) but involving 4 vertices (4-particle system).
- For the microstructure (a), no higher significance of the quadratic polynomial compared to the linear one can be detected whereas, at least in the bending
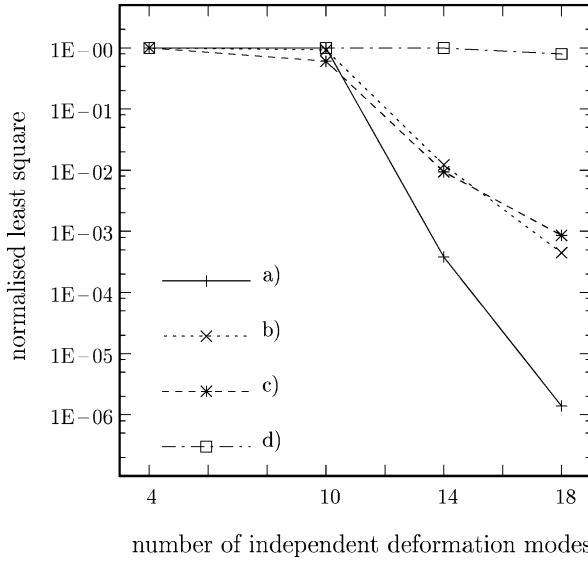
Fig. 11.4 Normalized least squares for several projection polynomials in the homogeneous tension experiment for the different microstructures at position ①. Whereas microstructure (*a*) shows a significantly decreasing error with increasing polynomial order, the decrease for (*b*) and (*c*) is less pronounced and it is nearly not observable for (*d*). Furthermore, the homogeneous deformation field does not account for differing accuracies due to the anisotropy of (*b*) and (*c*)
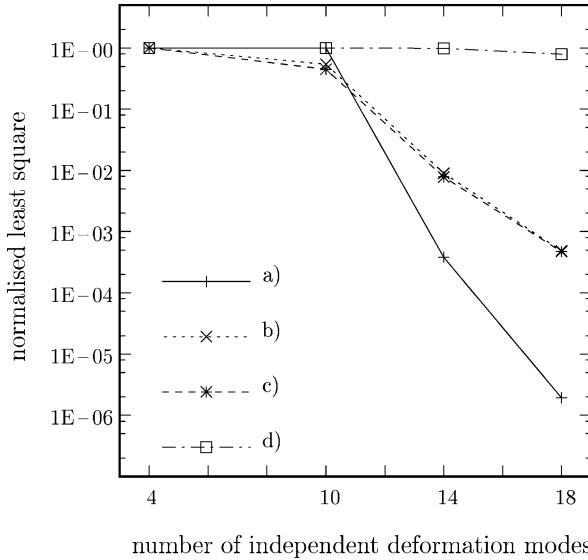
Fig. 11.5 Normalized least squares for several projection polynomials in the inhomogeneous shear experiment at the homogeneous position ②. Similar to the tension test, one can observe an dramatic decrease of the error for microstructure (*a*), a smaller but still significant decrease for (*b*) and (*c*). For (*d*), the extension to a cubic projection polynomial seems to influence the fitting accuracy only in a subordinate way
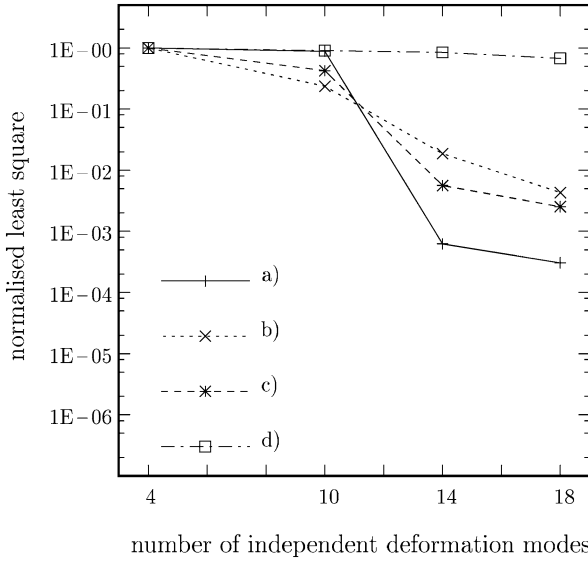
Fig. 11.6 Normalized least squares for several projection polynomials in the numerical shear experiment at the inhomogeneous position ③. Analogous to the homogeneous deformation states at ① and ②, one may observe the decrease of the error. Nevertheless, the difference between the micromorphic and the cubic polynomial is much less pronounced for microstructure (*a*). In contrast, the fitting accuracy for microstructures (*b*)–(*d*) is not seriously affected by the more inhomogeneous character of the deformation state. Merely the difference between (*b*) and (*c*) seems to be slightly more pronounced

experiment, the microstructures (b) and (c) respond to the quadratic, i.e., bending, deformation modes. This difference can be clarified taking into account the effective bending stiffnesses of the particular microstructures which depend, besides other effects, on the aspect ratio of the struts. Thus, one may expect a slightly higher effective bending stiffness for (b) and (c), $r \approx 1/12$, than for (a), $r \approx 1/20$. From the physical point of view, a low bending stiffness of the structure concentrates the bending effects close to the boundary. For (a), the bending modes decay within one layer of unit cells can not be detected at the investigated positions.

- A third point of interest is the relation between the micromorphic and the cubic polynomials at ③ and ④ for the microstructure (a). Obviously, the relevance of the complete cubic polynomial is less pronounced as it is at ① and ②.

To summarize the found observations, we want to conclude the proposed micromorphic projection rules to meet the real displacement fields of the reference computation in a significantly exacter way than the linear projection of a first order FE² approach does. However, the advantage of the higher order projection rules strongly depends on the topology within the investigated periodic unit cell, i.e., within the volume representative for the particular microstructure. In order to return to the analogy of vertices and particles, the present study indicates that for $(n > 1)$-particle
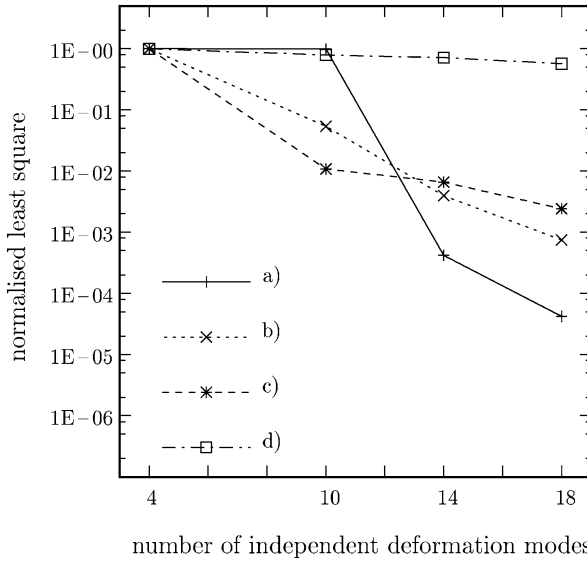
Fig. 11.7 Normalized least squares for several projection polynomials in the numerical bending experiment at position ④. Similar to position ③, the micromorphic and the cubic polynomials show a significantly higher accuracy for microstructure (*a*) than the linear and quadratic polynomials. The difference between the micromorphic and the cubic polynomials is less pronounced than at positions ① and ②. For (*b*) and (*c*), the fitting accuracy is obviously influenced by the microstructure's orientation

systems the microstructural degrees of freedom within the micromorphic continuum theory, i.e., the microrotation, the microdilatation, etc. loose their physical meaning. This result is in accordance to [16, 17] which have found similar properties identifying an effective Cosserat medium. Nevertheless, the micromorphic kinematics are able to reproduce the periodic 1-particle microstructure in a rather exact way, i.e., the deformation modes activated by the extended projection rule cover all essential deformation mechanisms of this particular microstructure. Furthermore, the second order homogenization methodology offers the fundamental advantage to reproduce size dependent boundary layer effects which has been verified in literature for several approaches, e.g., [9, 12, 13]. Thus, even assuming an arbitrary ($n > 1$)-particle system, the second order methodologies, the micromorphic as well as the second gradient approach, are a priori able to capture higher order effects. However, for the ($n > 1$)-particle case, we want to point out the present methodology to describe a phenomenological model beyond the straight interpretation based on the microtopology. Future investigations will focus on the polynomial coefficients found by the fitting technique. The question arises if one is able to restrict the full micromorphic medium to one of the subclasses proposed in [6] by an appropriate interpretation of those coefficients.

References

1. Cosserat, E., Cosserat, F.: Théorie des corps déformables. Hermann et Fils, Paris (1909)
2. Diebels, S., Steeb, H.: The size effect in foams and its theoretical and numerical investigation. Proc. R. Soc. Lond. A **458**, 2869–2883 (2002)
3. Eringen, A.C.: Microcontinuum Field Theories, vol. I: Foundations and Solids. Springer, New York (1999)
4. Feyel, F., Chaboche, J.L.: FE^2 multiscale approach for modelling the elastoviscoplastic behaviour of long fiber SiC/Ti composite materials. Comput. Methods Appl. Mech. Eng. **183**, 309–330 (2000)
5. Forest, S.: Homogenization methods and the mechanics of generalized continua—Part 2. Theor. Appl. Mech. **28**, 113–143 (2002)
6. Forest, S.: Nonlinear microstrain theories. Int. J. Solids Struct. **43**, 7224–7245 (2006)
7. Forest, S., Sab, K.: Cosserat overall modeling of heterogeneous materials. Mech. Res. Commun. **25**, 449–454 (1998)
8. Germain, P.: La méthode des puissances virtuelles en mécanique des milieux continus. Première partie: Théorie du second gradient. J. Mec. **12**, 235–274 (1973)
9. Jänicke, R., Diebels, S.: A numerical homogenisation strategy for micromorphic continua. Nuovo Cim. Soc. Ital. Fis. C **31**(1), 121–132 (2009)
10. Jänicke, R., Diebels, S., et al.: Two-scale modelling of micromorphic continua. Contin. Mech. Therm. **21**, 297–315 (2009)
11. Kouznetsova, V.G.: Computational homogenization for the multi-scale analysis of multi-phase material. PhD thesis, Technische Universiteit Eindhoven, The Netherlands (2002)
12. Kouznetsova, V.G., Geers, M.G.D., Brekelmans, W.A.M.: Size of a representative volume element in a second-order computational homogenization framework. Int. J. Multiscale Comput. Eng. **2**(4), 575–598 (2004)
13. Larsson, R., Diebels, S.: A second order homogenization procedure for multi-scale analysis based on micropolar kinematics. Int. J. Numer. Meth. Eng. **69**, 2485–2512 (2006)
14. Maugin, G.A.: Nonlocal theories or gradient-type theories: a matter of convenience? Acta Mater. **31**, 15–26 (1979)
15. Miehe, C., Koch, A.: Computational micro-to-macro transitions of discretized microstructures. Arch. Appl. Mech. **72**, 300–317 (2002)
16. Sab, K., Pradel, F.: Homogenisation of periodic Cosserat media. Int. J. Comput. Appl. Technol. **34**(1), 60–71 (2009)
17. Tekoglu, C., Onck, P.R.: Size effects in the mechanical behaviour of cellular materials. J. Math. Sci. **40**, 5911–5917 (2005)
18. Tekoglu, C., Onck, P.R.: Size effects in two-dimensional Voronoi foams: a comparison between generalized continua and discrete models. J. Mech. Phys. Solids **56**, 3541–3564 (2008)